第 25 卷第 2 期 无 机 化 学 学 报 Vol.25 No.2
2009 年 2 月 CHINESE JOURNAL OF INORGANIC CHEMISTRY 321~329

碳纳米管内分立的纳米铁粒子的热氧化性能研究

黄 钊 陈乾旺* 刘业如
(合肥微尺度物质国家实验室,中国科学技术大学材料科学与工程系,合肥 230026)

摘要: 研究了纳米铁填充的碳纳米管基复合纤维在空气中的热氧化性能。结果表明:一般在室温即被氧化的铁(Fe)纳米粒子在 170 ℃仍然具有良好的稳定性。这一方面是由于碳纳米管的保护作用所致,另一方面碳纳米管末端的 Fe 纳米粒子在室温下即迅速被氧化成反尖晶石型 Fe_3O_4/γ-Fe_2O_3,170 ℃以下能有效阻止氧分子向碳纳米管内扩散。因此,170 ℃可以被看作氧分子扩散进入碳纳米管腔的极限温度。在 170 ℃以下时,氧分子无法渗透 Fe_3O_4/γ-Fe_2O_3 晶格在管腔中形成氧分子。当温度高于 170 ℃时,氧分子渗透发生,管腔内的 Fe 纳米粒子由靠近管末端位置到内部逐渐被氧化。由于相对良好的热氧化稳定性,Fe 填充碳纳米管基复合纤维的铁磁性将可以在更高温度范围内得以保持。

关键词: 热稳定性; 碳"纳米试管"; 反尖晶石结构; 氧扩散; 临界温度
中图分类号: O613.71; O614.81+1 **文献标识码**: A **文章编号**: 1001-4861(2009)02-0321-09

Thermal Oxidation Mechanism of Fe Nano-particles Encapsulated Separately in Carbon Nanotubes

HUANG Zhao CHEN Qian-Wang* LIU Ye-Ru
(*Hefei National Laboratory for Physical Sciences at Microscale, Department of Materials Science & Engineering, University of Science & Technology of China, Hefei* 230026)

Abstract: Thermal oxidation of Fe nano-particles in nanoscopic reactors of carbon nanotubes (CNTs) was investigated by treatment in air from room temperature to 800 ℃. It is found that encapsulated Fe nano-particles are thermally stable up to a relatively high temperature of 170 ℃ comparing to oxidization at room temperature of bare ones. Fe nano-particles in the tube end of CNTs is easily oxidized to form inverse spinel structure Fe_3O_4/γ-Fe_2O_3 nano-particles, serving as barriers to prevent oxygen from diffusion into the inner hollow cavity of CNTs. It is suggested that 170 ℃ is the critical temperature (T_c) of oxygen diffusion through the barriers. At temperatures lower than 170 ℃, oxygen molecules can not diffuse through the lattice of Fe_3O_4/γ-Fe_2O_3 nano-particles to form oxygen molecules in the cavity of CNTs, while at higher temperatures the penetration of oxygen occurs and Fe nano-particles from the tip to inner most in CNTs are gradually oxidized. The mechanism is different from the oxidation behavior and thermal stability of a CNT-encapsulated Fe nanowire, which is oxidized continuously once the oxidation occured by oxygen ions migrating through the lattice of iron oxides and combines with Fe atoms to complete the oxidation process.

Key words: thermal stability; carbon "test tube"; inverse spinel structure; oxygen diffusion; the critical temperature

Ferromagnetic metallic nano-particles attract both fundamental and technological research interest for their prospective applications in various areas such as magnetic data storage, catalysis, xerography, magnetic

收稿日期:2008-10-09。收修改稿日期:2008-11-12。
国家自然科学基金(No.20125103)资助项目。
*通讯联系人。E-mail:cqw@ustc.edu.cn; Tel: 0551-3607292
第一作者:黄 钊,男,27 岁,博士研究生;研究方向:碳基材料的合成与应用。

resonance imaging, and biomedical applications[1~5]. However, the application is limited for their sensitivity to air oxidation as such nanometer-sized particles have larger surface area, offering the promise of enhanced reactivity, greater efficiency, and potentially new and unusual active sites[6]. For instance, a pristine surface of Fe exposed to air or oxygen-containing atmosphere is oxidized instantly at room temperature[7]. Moreover, ultrafine nano-particles of iron are pyrophoric[8]. Methods to protect the active material from early or undesired reactions are required if easy, cost-effective applications of these materials are to be realized. Carbon nanotubes (CNTs), possessing excellent properties such as uniform pores, good chemical stability, and large specific surface area, could be used as one of the coating materials to provide an effective barrier[1] against oxidation and consequently ensure a long-term stability of the metallic particles encapsulated[9~11]. Several successful applications were reported, including synthesis of metallic nano-particles (e.g., Fe, Cu, Ni and Fe-Nd-B)[12~15] in cavity of CNTs, making it possible to investigate magnetic, electronic and thermal properties of the novel structure of CNTs/metal nanocapsules[16~18].

Nanoscopic chemical and thermal behaviors of CNTs/metal nanocapsules are generally classified into two categories according to the role of carbon shell. One of them is: CNTs participate in reactions themselves. Bao et al.[19] developed a facile reduction of iron oxide/carbon nanotube encapsulates, using the carbon shell as reducing agent directly. In their work, the formation of metallic Fe was observed in the CNTs bores at the low temperature of 600 ℃ relative to the reduction of Fe_2O_3 at 800 ℃ on the outer surface of CNTs. The curvature-induced effects of nanotubes were employed to understand the facilitated reduction of Fe_2O_3, proving that nanotubes provide a confined environment with unique electronic properties. Chen et al.[20] made further studies on the nanoscopic reducing reaction of Fe_3O_4 to metallic Fe in a-CNT (amorphous carbon nanotube). It was revealed that gas such as hydrogen could not easily enter into a nanotube reactor to take part in reactions, because the barrier power of a-C∶H films was strongly increased by the occurrence of a network of cracks spread out over the whole a-C∶H surface.[21] At high temperatures, H_2 released from a-CNT shell tends to diffuse to exterior rather than cavity of the a-CNT shell. The other is: CNTs were inert in reactions, functioning only as templates or "test tubes". Han et al.[22] described the synthesis of $Fe_{3.5}B$ nanowires via boriding Fe nanowires encapsulated in CNTs, demonstrating that CNTs can be used as nanoreactors for changing the existing filling from one kind of material to another. Ilie et al.[23] studied the thermal stability and reactivity of oxidation of single-wall carbon nanotubes (SWCNTs) filled with metal halide nanowires. The activation energy for oxidation decreases considerably after filling, indicating that filled nanotubes are more amenable to controlled modifications based on chemical reactivity than the originating empty nanotubes.

It could be seen clearly that most of the reports are focusing on CNT-encapsulated continuous metallic nanowires. To the best of our knowledge, only a little theoretical attention is paid to thermal behaviors of separated metallic nano-particles encapsulated in CNTs, which would be more contributing to the specific thermal mechanism of nano-sized carbon "test tubes" via investigating changes of nano-particles at different positions in CNTs. Poulikakos et al.[24] studied the solidification and the structure of gold nano-particles in carbon nanotubes using molecular dynamics (MD) simulation, and found that the solidification temperature was higher than the corresponding unsupported clusters, practically depending only on the length of the nanoparticle. Very recently, Wang et al.[25] used the Monte Carlo simulation to investigate the thermal evolution of the icosahedral Pt_{55} clusters encapsulated in SWCNTs. Their results indicated that the melting-like transformation temperature of the icosahedral Pt_{55} clusters encapsulated in SWCNTs increased with the pore size of SWCNTs, which had a significant effect on the structures of the encapsulated icosahedral Pt clusters. However, intuitive experimental evidences on thermal behavior of CNT-encapsulated metallic nano-particles become the urgent need at present. In this work, we present a detailed investigation on the oxidizing behavior of Fe nano-particles with diameters of 20~30 nm sepa-

rately encapsulated in the cavity of CNTs. Our results show that inverse spinel structure Fe_3O_4/γ-Fe_2O_3 nanoparticles formed in the tube end of CNTs can effectively prevent oxygen from diffusing into the inner hollow cavity of CNTs at temperatures below 170 ℃ and protect the inner Fe nano-particles from being oxidized.

1 Experimental

In a typical procedure, the reaction was carried out by heating 1.00 g of ferrocene and 6.0 g of dry ice in a 20 mL steel autoclave at 400 ℃ for 800 min. After cooling down to room temperature, the dark brown product was washed with toluene and ethanol, respectively, then dried at 110 ℃ for 3 h to obtain Fe_3O_4/a-CNT coaxial nanocables[26]. The heat treatment of the boat was performed by a tube furnace in N_2 stream, with a flow rate of 100 mL·min^{-1}. Heating-up rate of the system was 10 ℃·min^{-1}, and the temperature was held for 30 min at 620 ℃. Agglomerated iron nano-particles encapsulated in carbon nanotubes accompanied with the crystallization of the a-CNT shell were the as-prepared products[20]. Finally, heat treatment of the as-prepared products was taken in quartz boat by a tube furnace in ambient air with a temperature ramp of 1 ℃·min^{-1}, and the temperature was held for 30 min at 150, 200, 250, 300, 350, 400 ℃, respectively. For comparison, another portion of the as-prepared products was held for 4 h when at 300 ℃ to understand the mechanism. Solid products were saved for further characterizations.

Thermal gravity analysis (TGA) and differential thermal analysis (DTA) were performed on DTG-60H thermal analyzer at the heating rate of 1 K·min^{-1} from room temperature to 800 ℃ in ambient air. Mass spectrometry was performed on Agilent 6890 GCT Micromass spectrometer. In mass spectrometry analysis, a sample was firstly held for 3 min at 30 ℃ for creating a vacuum environment, then heated to 100 ℃ at the heating rate of 100 ℃·min^{-1} and held for another 3 min, finally heated to 180 ℃ at the heating rate of 80 ℃·min^{-1} and held for 3 min. The powder X-ray diffraction(XRD) analyses were performed on a Rigaku D/MAX-rA X-ray diffractometer equipped with Cu $K\alpha$ radiation (working voltage 40 kV, working current 100 mA, λ = 0.154 18 nm) over the 2θ range of 10°~70°. After light splitting by the graphite monochromator accompanied with a PHA analyzer, X-rays are recorded by scintillation counter, using 2θ-θ linkage symmetry scanning mode. SEM images were taken on JSM-6700F field emission scanning electron microscopy. TEM analyses were performed on a Hitachi H-800 Transmission Electron Microscope and the accelerating potential is 200 kV. High-resolution transmission electron microscope(HRTEM) images were taken on JEOL-2010 with an accelerating voltage of 200 kV.

2 Results and discussion

2.1 Macrocosmic measurements of thermal oxidation of the sample by TG/DTA analysis

The thermal stability of the carbon-encapsulated Fe nano-particles (black powder) was investigated by TG/DTA measurements in ambient air(Fig.1). Reddish powder was collected as residual product after cooling down. TG and DTA curves indicate that the thermal variation of the as-prepared products involves six stages, marked A-F in Fig.1. Phenomenon and mechanism in these stages will be discussed later.

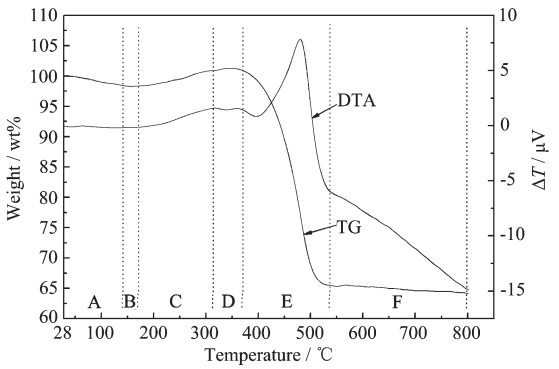

Fig.1　TG and DTA curves of the carbon-encapsulated Fe nano-particles carried out at the heating rate of 1 ℃·min^{-1} in air environment. A~F indicates the six stages of thermal variation of the specimen

Fig.2 displays SEM and TEM images of the as-prepared products before heat treatment, heated to 300 ℃ and 400 ℃, respectively. It can be seen from TEM images that the majority of Fe nano-particles in carbon nanotubes are in diameters of 20~30 nm. No obvious changes in morphology are observed between either SEM images of a1 and b1, or TEM images of a2 and b2,

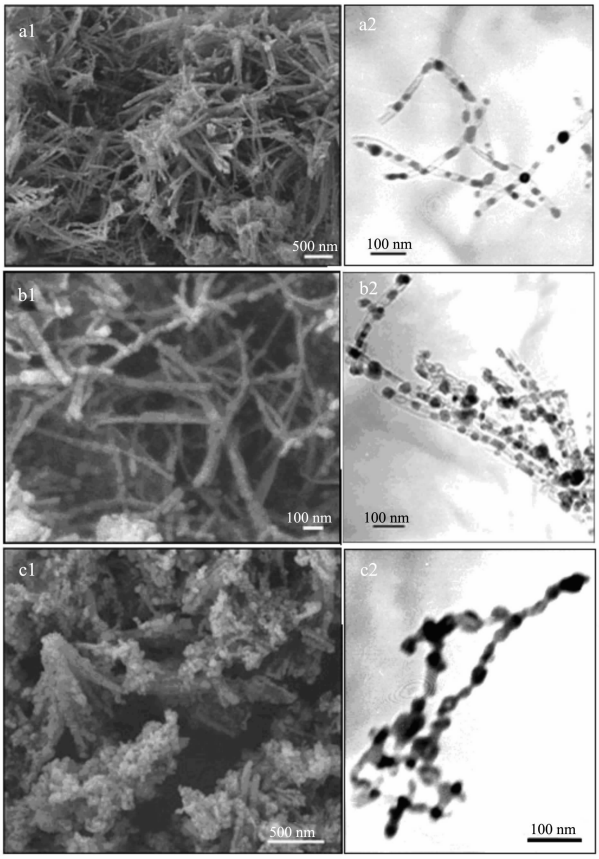

Fig.2 SEM and TEM images of (a) the as-prepared products and the carbon-encapsulated Fe nano-particles after heated to temperatures of (b) 300 ℃ and (c) 400 ℃. Fe_3O_4/a-CNT nanocables was taken in quartz

exhibiting stability of this nanocapsule structure below 300 ℃. Images c1, c2 reveal that some carbon shells are expelled after burning in air environment when the temperature is increased to 400 ℃, which is confirmed by TG-DTA analysis. Aligned nano-particles are left as residues.

XRD patterns in Fig.3 reveal the variation of the specimen in each stage of TG-DTA measurements. Fig. 3a shows typical graphite and α-Fe(PDF 87-0722) as the dominating phase, with Fe_3O_4(PDF 85-1436) and γ-Fe_2O_3(PDF 04-0755) as impurity phases[27]. Fig.3b, 3c reveal the intensity increase of Fe_3O_4/γ-Fe_2O_3 peaks, indicating continuous transition of α-Fe to Fe_3O_4/γ-Fe_2O_3 with the temperature. Another phase of α-Fe_2O_3 (PDF 89-2810) appears when the temperature comes up to 300 ℃, indicating transition of nanocrystalline magnetite (Fe_3O_4) and maghemite (γ-Fe_2O_3) to hematite (α-Fe_2O_3) (as shown in Fig.3d, e)[28]. Finally, Fig.3f reveals

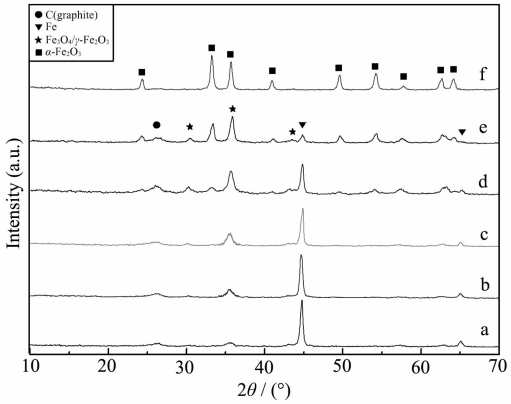

Fig.3 XRD patterns of the carbon-encapsulated Fe nano-particles heated to tempretures of (a) 150 ℃, (b) 200 ℃, (c) 250 ℃, (d) 300 ℃, (e) 350 ℃ and (f) 400 ℃ and then cooled down in ambient air. Peaks of the compounds were labeled on the patterns

typical peaks of exclusive α-Fe_2O_3. Phases of graphite, α-Fe and Fe_3O_4/γ-Fe_2O_3 disappear, indicating complete reaction occurrs with α-Fe_2O_3 left over.

In order to confirm the critical temperature of oxygen diffusion through the iron oxide barriers found in TG/DTA analysis. Mass spectra is shown in Fig.4. It is observed that no CO_2 is detected in the time of 10.7 min, indicating no CO_2 desorbs from the sample in the whole heating process to 180 ℃. On the other hand, the amount of H_2O vapor decreases in the first 3 min, attributed to the pump for vacuum environment. Although a slight peak in the time interval 3 ~3.7 min shows the fully desorption of H_2O vapor on the surface of the sample below 100 ℃, the intensity is invariable

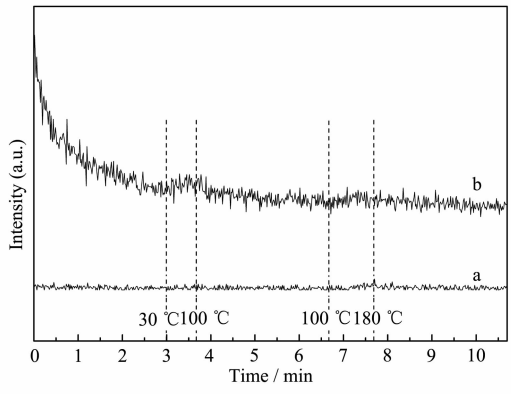

Fig.4 Mass spectra of (a) CO_2 and (b) H_2O vapor desorption with the time extended. Temperatures of 30 ℃, 100 ℃ and 180 ℃ were labeled at corresponding time by dash lines

afterwards, indicating that no H_2O vapor desorbs from the sample in the temperature interval of 100~180 ℃. Hence, the variation of TG/DTA curves at the temperature of 170 ℃ could be attributed to the oxidation of encapsulated Fe nano-particles due to the oxygen diffusion through the iron oxide barriers, but neither desorption of CO_2 nor H_2O vapor, which does not allow us to draw a definite conclusion.

Based on the characterization results of SEM, TEM and XRD, each stage of TG/DTA measurements could be briefly accounted for in Table 1. Below 141 ℃, the endothermic process is attributed to the release of adsorbed gases and moisture on the surface of the nanocapsules. The weight increase in the temperature interval of 170~314 ℃ is related to oxidation of α-Fe to the phase of Fe_3O_4/γ-Fe_2O_3. Besides, magnetite (Fe_3O_4) nano-particles tend to transform into the fully oxidized, cation deficient oxide maghemite (γ-Fe_2O_3), since the Fe^{2+} cations are not stable upon exposure to oxygen-containing atmosphere. When the temperature comes up to 314 ℃, transition of metastable maghemite(γ-Fe_2O_3) to hematite(α-Fe_2O_3) occurs, while remaining Fe nano-particles oxidized unceasingly. Finally in the temperature interval of 372~536 ℃, the weight decrease is accompanied by exothermic reactions and can be ascribed to the burning of the carbon coatings, with the ultimate oxides consisting of agglomerated hematite(α-Fe_2O_3) nano-particles aligned in lines. According to the experimental results, one clear sees that Fe nano-particles encapsulated in CNTs exhibit thermal stability below 170 ℃. Complete oxidation even occurs above 350 ℃. In contrast, bare iron nano-particles can be oxidized in a minute even at room temperature with the generation of oxide layers about 2 nm on the surface[29]. Moreover, according to Caberra-Mott model of oxidation, 110 ℃ is the threshold temperature at which bare Fe nano-paricles in diameter about 20 nm is completely oxidized under oxygen partial pressure of 267 Pa. Apparently, Fe nano-particles encapsulated in CNTs exhibit much better thermal stability than bare ones, attributed to effective protection of carbon shells. The results contribute a lot to the prospective application of the fantastic ferromagnetic material.

Table 1　Description of phenomena in each stage of TG-DTA measurements of Fig.1

Stage	Temperature Range / ℃	Mass variation / wt%	Heat variation	Corresponding XRD patterns[a]
A	28-141	−1.66	Endothermic	N/A
B	141-170	0	Invariable	a
C	170-314	+2.52	Exothermic	b, c, d
D	314-372	+0.48	Exothermic	e
E	372-536	−35.57	Exothermic	f
F	536-800	0	Invariable	N/A

[a] XRD patterns mentioned in the table are corresponding to those in Fig.3

2.2　Oxidative behavior of microscopic Fe nano-particles in CNTs based on HRTEM characterizations

Although the XRD patterns in Fig.3 have already revealed the oxidation behavior of inner Fe nano-particles along with the temperature increase, which offers a statistical average result, we have performed detailed characterization of some particular carbon-encapsulated Fe nano-particles heated to different temperatures by HRTEM images to study the oxidizing process of Fe nano-particles in these nanometer-sized carbon test tubes along with XRD analysis. Two independent groups of particles were investigated, and one typical group of them is presented in this report after heated to 150, 250 and 400 ℃, respectively (Fig.5) (HRTEM analysis of another nanotube encapsulating three particles heated to 150 ℃ can be found in Supporting Information). The fast Fourier transform(FFT) pattern, calculated from the HRTEM image, reveals symmetry of corresponding nano-particle. Some of them appear simultaneously to be several groups of dot arrays, for the selected nano-particles are agglomerated with several nanocrystals. However, HRTEM analysis of d value could be employed to confirm the structure of different

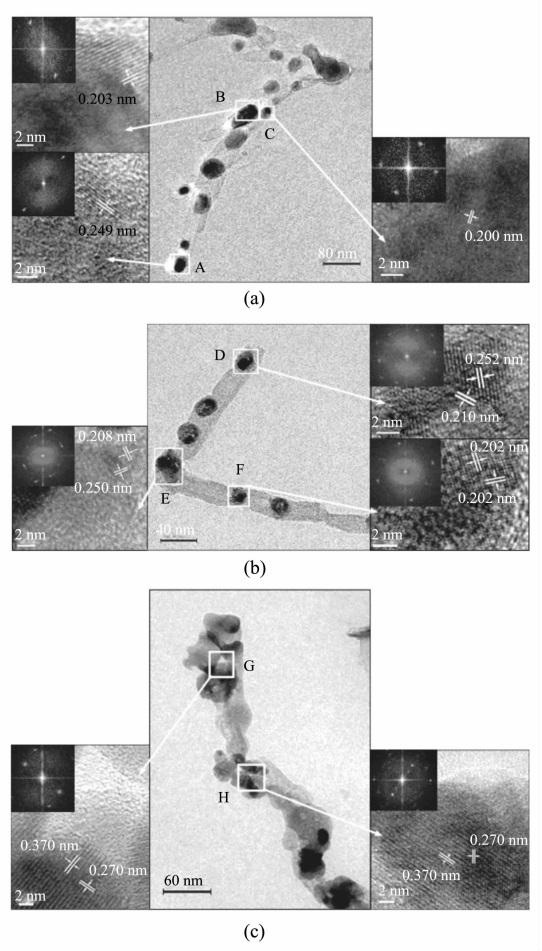

Fig.5 HRTEM images of the carbon-encapsulated Fe nano-particles heated to tempretures of (a) 150 ℃, (b) 250 ℃, (c) 400 ℃. The insets show the fast Fourier transform(FFT) pattern corresponding to the HRTEM image

nano-particle in a single carbon nanotube. Fig.5a displays HRTEM images of a single carbon nanotube and three encapsulated nano-particles heated to 150 ℃. Left lower image(particle A in the tube end of CNT) reveals *d* spacing of 0.249±0.005 nm(Stat. 10 spacing), corresponding to the [311] plane of Fe_3O_4/γ-Fe_2O_3. Apparently, particle A is oxidized from α-Fe, consisting of dominantly Fe_3O_4 and γ-Fe_2O_3 in small quantities considering the core size(>20 nm).[30] Left upper image(particle B in the cavity but near to the open tip of CNT) reveals d spacing of 0.203±0.005 nm, while right image (particle C in the very interior of CNT) reveals d spacing of 0.200±0.005 nm, all corresponding to the [110] plane of α-Fe. It can be concluded from Fig.5a that oxygen molecules in air are unable to enter into the cavity of CNT and inner Fe nano-particles are not oxidized due to some effective barriers at 150 ℃. Combined with XRD analysis of Fig.3a, weak peaks of Fe_3O_4/γ-Fe_2O_3 are induced by the oxide shells of nano-particles located at the exterior and in the tube end of CNTs. None of inner Fe nano-particles is oxidized to the phase of Fe_3O_4/γ-Fe_2O_3 before heated to 170 ℃.

HRTEM images of a single carbon nanotube and three encapsulated nano-particles heated to 250 ℃ are shown in Fig.5b. *d* spacing of 0.252±0.005 nm and 0.210±0.005 nm of two-dimensional lattice fringes, corresponding to the [311] and [400] planes of Fe_3O_4/γ-Fe_2O_3, indicates complete oxidation of particle D in the tube end of CNT (right upper image). Furthermore, *d* spacing of 0.250±0.005 nm and 0.208±0.005 nm of two-dimensional lattice fringes, corresponding to the [311] and [400] planes of Fe_3O_4/γ-Fe_2O_3, indicates oxidation of particle E in the cavity of CNT (left image). However, *d* spacing of 0.202±0.005 nm of two-dimensional lattice fringes, corresponding to the [110] plane of α-Fe, indicates that particle F in deeper cavity of CNT is consisted of exclusive unoxidized Fe(right lower image). In addition, XRD pattern of Fig.3b shows typical intensity increase for Fe_3O_4/γ-Fe_2O_3 peaks, indicating transition of inner α-Fe particles to Fe_3O_4/γ-Fe_2O_3 when the temperature increases to 200 ℃. Obviously, oxygen molecules have entered into the cavity of CNTs and oxidized inner Fe nano-particles before the temperature comes up to 200 ℃. Meanwhile, Fe nano-particles in deeper cavity get lower level of oxidization. Since the carbon shells are structurally and thermally stable, it is generally accepted that they are not favorable for oxygen permeating, oxygen molecules are more likely to diffuse through the inverse spinel structure Fe_3O_4/γ-Fe_2O_3 nano-particles in the tube ends and enter into the nanotubes.

HRTEM images of the specimen heated to 400 ℃ are shown in Fig.5c. It is found that carbon nanotubes in the figure burn out, with residual nano-particles aligning tightly. *d* spacing of 0.270±0.005 nm and 0.370±0.005 nm of two-dimensional lattice fringes of particle G and H corresponds to the [104] and [012] planes of α-Fe_2O_3. Fe nano-particles have been fully

oxidized, with generated Fe_3O_4/γ-Fe_2O_3 transforming to α-Fe_2O_3, which agrees with XRD pattern of Fig.3f.

2.3 Oxidative mechanism

A model is proposed to understand the oxidization mechanism of Fe nano-particles encapsulated separately in CNTs(Fig.6). In the beginning, Fe nano-particle in the tube end of CNTs is easily oxidized to Fe_3O_4/γ-Fe_2O_3 at low temperatures. Dissociative adsorption of oxygen in air occurs on the surface of the iron oxide nano-particle in the tube end for the high oxygen partial pressure there, and then oxygen ions migrate along the oxygen vacancies of the nano-particle. However, at such low temperatures, oxygen ions can not desorb and combine as oxygen molecules at the lower oxygen partial pressure side in the cavity of CNT. Hence, Fe nano-particles inside the CNTs are safely protected(as shown in Fig.6a). The inverse spinel structures for oxygen permeating membrane has seldom been reported directly. However, Lee et al.[31] found that the oxygen permeability of dense oxygen permeable perovskite-type ceramic membranes, $La_{0.7}Sr_{0.3}Ga_{0.6}Fe_{0.4}O_{3-\delta}$, were enhanced 6 times by introducing nanosized surface reactive layers, $La_{0.6}Sr_{0.4}CoO_{3-\delta}$ on the surface of oxygen ion transport membranes. The enhancement may have been caused both by the increase in the effective surface area and by the increase in surface activity to oxygen dissociation and association when the nanosized layers are introduced. Another work by Jin et al. reported the oxygen permeation flux of $SrCo_{0.4}Fe_{0.5}Zr_{0.1}O_{3-\delta}$ via a flame aerosol synthesis(FAS) method was increased by 40% at the elevated temperatures comparing to that via the traditional solid-state reaction(SSR) method[32]. Because SSR method sets an insurmountable barrier to fabricate nanosized MIEC oxides, while FAS method often ensures the formation of the perovskite-type oxides with nanostructures. All these suggest when the grain size is decreased to nanometer scale, oxygen permeability could be greatly enhanced. It is suggested that the mechanism is also applicable to inverse spinel structures in this report, although they typically display low oxygen permeability. The oxygen succeeds in permeating the Fe_3O_4/γ-Fe_2O_3 nano-particles with a size of 20~30 nm. When the temperature elevates to 170 ℃ (according to the TG-DTA analyses), the inverse spinel iron oxide particles are no longer barriers against oxygen penetration as bulk ones. Oxygen succeeds in diffusing through the iron oxide nano-particle in the tube end and desorbs as oxygen molecules in the cavity, then arrive at the second Fe nano-particle rapidly to oxidize it (as shown in Fig.6b)[33]. With the temperature elevation, oxygen increases its diffusivity and diffuses slowly in the cavity to gradually oxidize Fe nano-particles from tip to inner most of CNTs in the oxidizing process(as shown in Fig. 6c). Obviously, temperature plays a very important role in oxygen diffusion through Fe_3O_4/γ-Fe_2O_3 nano-particles and oxidation of Fe nano-particles in the cavity of CNTs.

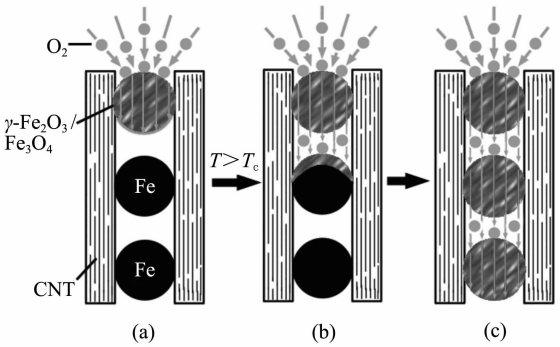

(a) below T_c, oxygen in air can not penetrate the inverse spinel structure Fe_3O_4/γ-Fe_2O_3 nano-particle in the tube end of CNT, though oxygen ions are able to migrate along the vacancies. Inner Fe nano-particles are safely protected. (b) when the temperature comes up to T_c, oxygen ions diffuse through the lattice of Fe_3O_4/γ-Fe_2O_3 nano-particle in the tube end and desorb as oxygen molecules in the cavity, then arrive at the second Fe nano-particle rapidly to oxidize it on the surface; (c) With the temperature elevated, Fe nano-particles are gradually oxidized by penetrated oxygen molecules from the tip to inner most of CNT.

Fig.6　A model for understanding the mechanism of nanoscopic oxidizing reaction in CNTs

Additional XRD patterns of the product holding for 30 min and 4 h at 300 ℃, respectively, are performed in order to get rid of time influence to oxygen diffusion in CNTs (Fig.7). There exists no obvious difference between respective peaks of a and b pattern, indicating Fe nano-particles does not get continuously oxidized with the time increase once the temperature is invariable. It can be easily understood that at certain temperatures, the amount of oxygen molecules is constant after quick permeation through Fe_3O_4/γ-Fe_2O_3 nano-particles in very short time. Oxygen pressure in the cavity of CNTs is invariable and residual Fe nano-particles are hardly oxidized along with the time, which agrees with the early report.[29] As a result, time influence to oxygen diffusion in CNTs is weak and neglectable during the whole process of oxidation.

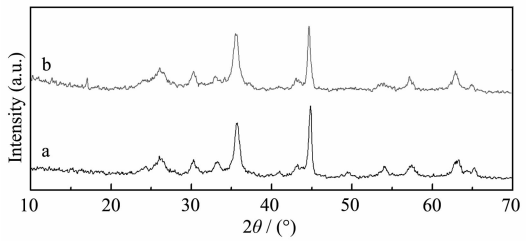

Fig.7 XRD patterns of the carbon-encapsulated Fe nano-particles heated to 300 ℃ and held for (a) 30 min, (b) 4 h, then cooled down in ambient air

Comparing with other nano-sized reaction in carbon nanotubes, the mechanism makes unique contribution, for the metallic nano-particles are encapsulated separately, much different from continuous nanowires in other reports. The temperature of 170 ℃, is especially described as the critical temperature, at which oxygen molecules can just diffuse through the inverse spinel structure Fe_3O_4/γ-Fe_2O_3 nano-particles in the tube end of CNTs and begin to oxidize inner Fe nano-particles. With the temperature elevatation, oxygen diffuses slowly in the cavity and gradually oxidizes Fe nano-particles from the tip to inner most of CNTs, different from the thermal behavior of a CNT-encapsulated nanowire, which is oxidized continuously once the oxidation occurred. For instance, ref. 22 has presented an oxidative behavior of continuous Fe nanowires encapsulated in CNTs. At high temperatures, B_2O_3 vapor entered carbon nanotubes interiors and started to oxidize the Fe nanowire continuously to form $Fe_{3.5}B$ nanowires in the tubes with the help of nitrogen. The difference is probably related to the way oxidative gas diffuses. In the oxidizing process of a CNT-encapsulated Fe nanowire, oxygen ions migrate through the lattice of iron borides or oxides and combine with Fe atoms to complete the oxidation process. But in this report, it is involved that oxygen penetrated the iron oxide nano-particles to form oxygen molecules and diffused in the cavity of CNTs. It is found that oxygen permeability is enhanced when the size of the inverse spinel structure iron oxide particles decrease to nanometer scale, no longer being barriers for oxygen diffusion as corresponding bulk materials. After a Fe nano-particle in the cavity is oxidized, oxygen could only diffuse through it when oxygen partial pressure is increased sufficiently at one side. As a result, the oxidizing reaction in the cavity is mild. Accordingly, the temperature range, over which the inner Fe nano-particles completely evolve into oxides, is supposed to be much wider than Fe nanowires encapsulated in CNTs with the same lengths.

3 Conclusions

We have shown that Fe filled carbon nanocapsules are thermally stable in air environment up to 170 ℃, which is suggested to be the critical temperature for oxygen diffusing through the inverse spinel structure Fe_3O_4/γ-Fe_2O_3 nano-particles in the tube end of CNTs by the oxidation of Fe nano-particles. Above 170 ℃, separate inner Fe nano-particles are gradually oxidized from tip to inner most, attributed to the diffusion of oxygen in the cavity of CNTs with the temperature elevation. The studies reveal that oxygen entering into a nanotube reactor to take part in reactions is determined by the oxygen permeability of nano-particles at the tip end.

Acknowledgement: This work was supported by the Natural Science Foundation of China(No. 20125103).

References:

[1] Kodama R H. *J. Magn. Magn. Mater.*, **1999**,**200**:359~372

[2] Oku T, Hirata T, Motegi N, et al. *J. Mater. Res.*, **2000**,**15:**

2182~2186

[3] Zhang H Y, Chen J, He Y Y, et al. *Mater. Chem. Phys*., **1998**, **55**:167~170

[4] Song H H, Chen X H. *Chem. Phys. Lett*., **2003**,**374**:400~404

[5] Bystrzejewski M, Huczko A, Lange H. *Sensors Actuat. B*, **2005**,**109**:81~85

[6] Bunker C E, Kames J J. *J. Am. Chem. Soc*., **2004**,**126**:10852~10853

[7] Fromm E. *Kinetics of Metal-Gas Interactions at Low Temperature*: *Hydriding, Oxidation, Poisoning*, Berlin: Springe, **1998**.63975

[8] Giri S, Ganguli S, Bhattacharya M, Appl. Surf. Sci., **2001**,**182**: 345~349

[9] Che G L, Lakshmi B B, Martin C R, et al. *Langmuir*, **1999**,**15**: 750~758

[10]Ajayan M, Lijima S. *Nature*, **1993**,**361**:333~334

[11]Tsang S C, Harris P J F, Green M L H. *Nature*, **1993**,**362**: 520~522

[12]Che R C, Peng L M, Duan X F, et al. *Adv. Mater*., **2004**,**16**: 401~405

[13]Choi W Y, Kang J W, Hwang H J. *Phys. Rev. B*, **2003**,**68**: 193405~193409

[14]Bao J C, Wang K Y, Xu Z, et al. *Chem. Commun*., **2003**,**2**: 208~209

[15]Bystrzejewski M, CudziłS, Huczko A, et al. *J. Alloys Compd.* **2006**,**423**:74~76

[16]Su Y C, Hsu W K. *Appl. Phys. Lett*., **2005**,**87**:233112-1~233112-3

[17]Muhl T, Elefant D, Graff A, et al. *J. Appl. Phys*., **2003**,**93**: 7894~7896

[18]Braidy N, Botton G A, Adronov A. *Nano Lett.*, **2002**,**2**:1277~1280

[19]Chen W, Pan X L, Willinger M, et al. *J. Am. Chem. Soc*., **2006**, **128**:3136~3137

[20]Cao F Y, Zhong K F, Gao A M, et al. *J. Phys. Chem. B*, **2007**, **111**:1724~1728

[21]Vasquez-Boruchi S, Jacob W, Achete C A. *Diamond Relat. Mater*., **2000**, **9**: 1971~1978

[22]Han W Q, Kohler-Redlich P, Scheu C, et al. *Adv. Mater*., **2000**,**12**:1356~1359

[23]Bendall J S, Ilie A, Welland M E, et al. *J. Phys. Chem. B*, **2006**, **110**:6569~6573

[24]Arcidiacono S, Walther J H, Poulikakos D, et al. *Phys. Rev. Lett.*, **2005**,**94**:105502~1~105502~4

[25]Cheng D J, Wang W C, Huang S P. *J. Phys. Chem. C*, **2007**, **111**:1631~1637

[26]Cao F Y, Chen C L, Wang Q, et al. *Carbon*, **2007**,**45**:727~731

[27]Kuhn L T, Bojesen A, Timmermann L, et al. *J. Phys.: Condens. Matter*, **2002**,**14**: 13551~13567

[28]Schimanke G, Martin M. *Solid State Ionics*, **2000**,**136**:1235~1240

[29]Linderoth S, Morup S, Bentzon M D. *J. Mater. Sci*., **1995**,**30**: 3142~3148

[30]Signorini L, Pasquini L, Savini L, et al. *Phys. Rev. B*, **2003**, **68**:195423~1~195423-8

[31]Lee K S, Shin T H, Lee S W, et al. *J. Cera. Proc. Res*., **2004**, **5**:143~147

[32]Wu Z T, Dong X L, Jin W Q, et al. *J. Mem. Sci*., **2007**,**291**: 172~179

[33]Chen H B, Johnson J K, Sholl D S. *J. Phys. Chem. B*, **2006**, **110**:1971~1975